

# Progress on Photon Counting Intensified APS

Michela Uslenghi<sup>a</sup>, Giovanni Bonanno<sup>b</sup>, Massimiliano Belluso<sup>b</sup>, Antonio Calì<sup>b</sup>, Cristina Timpanaro<sup>b</sup>, Rosario Cosentino<sup>b</sup>, Salvatore Scuderi<sup>b</sup>, and Angelo Modica<sup>c</sup>.

<sup>a</sup>Istituto di Astrofisica Spaziale e Fisica Cosmica - CNR, Via Bassini, 15, Milano, ITALY

<sup>b</sup>Osservatorio Astrofisico di Catania, Via S. Sofia 78, 95123 Catania, ITALY.

<sup>c</sup>Xilinx Ireland, Logic Drive, Citywest Business Campus, Saggart, Dublin, IRELAND

## ABSTRACT

We report on the progress of the activity, started one year ago, to obtain a photon counting, MCP-based detector, optimized for high count-rate. A new electronic board, hosting both the APS and the electronics processing unit, has been developed. The new architecture of the system, designed to drive the detector, to acquire the images and compute the photon event centers, is described in detail in this paper. We also report the functional tests carried out on the sub-parts of the detector along with a preliminary characterization of the system.

**Keywords:** UV Detectors, Intensifiers, Intensified CMOS-APS, Microelectronics, Astronomy

## 1. INTRODUCTION

MCP based detectors are the most commonly used Ultraviolet photon counting devices for astronomy<sup>1,2,3,4,5</sup>, due to the high quantum efficiency (depending on the wavelength range even more than 50%), solar blindness, low background ( $< .1 \text{ counts/s}\cdot\text{cm}^2$ ), large format ( $> 2000 \times 2000$  pixels), high resolution in space ( $< 15 \mu\text{m}$ ) and time (down to  $\sim 0.1 \text{ ns}$ ). Several readout systems have been developed depending on the particular application, each one allowing exploiting one or several characteristics of the MCP intensifiers. Photon Counting Intensified CCDs<sup>6,7,8,9,10</sup> (PC-ICCDs), in particular, which use a fast scan CCD as a readout system, exhibit the best spatial resolution (better than  $3 \mu\text{m}$ ), well higher than that allowed for the MCP currently available. Thus, the resolution of the PC-ICCDs is now limited by the intensifier, but the newly developed Silicon MCP<sup>11</sup> will likely offer, among a number of other advantages (lower background, wider choice of photocathodes, larger area, better uniformity), smaller pore diameter (down to  $2 \mu\text{m}$ ).

Moreover, PC-ICCD presents a very modular architecture allowing optimizing independently the head and the readout system for different kinds of applications.

The main limitation of the PC-ICCD is the low local dynamic range, which is limited by the frame rate: in fact, photon events overlapping within a single CCD frame period are lost. In order to overcome this problem, keeping the main characteristics of an optical readout-based photon counter, we started to develop a Microchannel Plate detector using a CMOS Active Pixel detector instead of a CCD. This sensor is a relatively new device, at the moment not yet exploited in scientific applications due to the low image quality. However, for this particular application we do not need high cosmetic characteristics, instead the high readout speed, resulting from the intrinsically parallel architecture, together with the reduced electronics complexity required to control the device (APS can be driven by digital circuitry and the A/D converter can be integrated on the chip, in which case both the input and the output signals are digital), could allow us a substantial improvement on the similar Intensified CCDs with a less complex electronics.

A first prototype has been realized using prototyping and commercial boards<sup>12,13</sup>. The aim was to test the feasibility of the project, but substantial improvements are required in order to exploit the characteristics of the APS sensor. In this framework we started the development of a new version of the electronics in order to run the APS at higher frequencies, keeping a reasonable level of noise.

## 2. DETECTOR OVERVIEW

The detector architecture is reported in Fig.1. A Z-stack MCP intensifier, operating in the saturated regime, produces a spot of several millions of optical photons on a phosphor screen for every photon detected. Then a CMOS APS, optically coupled to the phosphor screen, records the image. A dedicated digital processing unit analyzes each frame, searches for valid events and computes the relative coordinates.

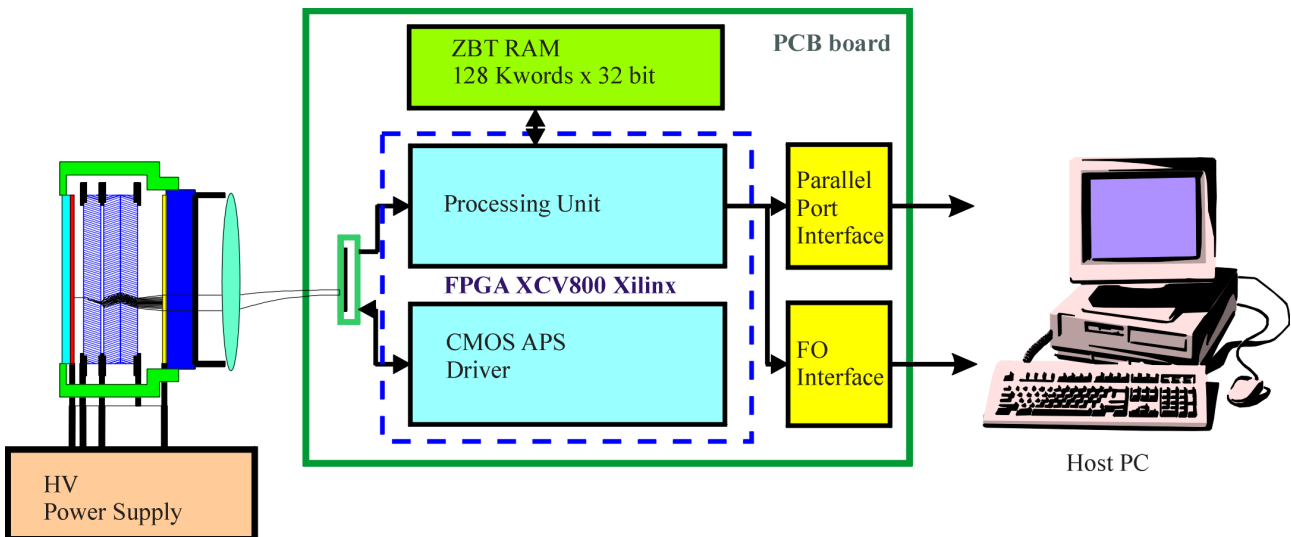


**Figure 1.** Block Diagram of the PC-IAPS.

The image intensifier used is a sealed Z-stack intensifier produced by Photek (MCP340), based on 40 mm diameter plates with 10  $\mu\text{m}$  pores at 12  $\mu\text{m}$  pitch. A P20 phosphor screen is deposited on a fiber optic (FO) faceplate. A RbTe photocathode, deposited on a  $\text{MgF}_2$  input window allows improving the quantum efficiency in the classical ultraviolet.

The electron cascade generated by the MCP stack is transduced, via a phosphor screen and a relay optical system (an HR-Heligaron 35 objective manufactured by Rodenstock, with a numerical aperture of 0.32) with 1:4.3 demagnification ratio onto the APS array, a Photobit PB-1024, with 10  $\mu\text{m}$  square pixel ( $6 \times 9 \mu\text{m}^2$  active area<sup>14</sup>) and 1024×1024 pixels format. This sensor, due to the 1024 8 bit A/D converters integrated on the chip and the eight parallel digital output ports, is able to provide up to 500 frames/s full frame and allows windowing with random access of the rows<sup>15</sup>.

The APS is mounted on a PCB board, which also hosts the driving electronics, the real time data processing unit and the interfaces to the host PC. The core of the electronics is a single FPGA, allowing a very compact design.

The architecture of the FPGA based digital data processing system is similar to that described in our previous papers<sup>12,13</sup>. The unit acquires the eight digitized outputs of the APS as to generate, through a proper system of delays, 3×3 pixel windows that sweep dynamically the whole APS matrix at the pace of the pixel clock. The processing system performs in parallel the following tasks on each window:

- check, according to appropriate discrimination and pile-up rejection criteria, for the presence of a charge distribution representing a photon event;
- compute the centroid coordinates with a resolution of 1/32 of a pixel, applying a simple center of gravity algorithm to the charge distribution in the current window. The centroid coordinates of the charge distribution identified as a photon event are subsequently transferred to the memory of the PC.

Two detector operating modes have been implemented:

1. a ‘frame grabber mode’, where the frames, as they are generated by the APS, are stored in a RAM memory and then transferred, using a slower data rate, to the memory of the host PC;
2. a ‘centroding mode’, where the collected photons are recorded in real-time as a list of event coordinates in series with tags marking the end of each frame; off-line data processing allows to compute the actual photon time tags from the frame number associated with each event, providing the time coordinate.

The software for data acquisition and detector control has been written in C, whereas the programs for the data analysis have been developed in Interactive Data Language (IDL).

### 3. ELECTRONICS BOARD

The detector electronics is implemented in a 10 cm x 10 cm PCB board (picture in Fig.2), hosting the APS CMOS and a single FPGA XILINX XCV800 (800 Kgates equivalent). The diagram is shown in Fig.3. It includes three main blocks:

- the CMOS APS controller
- the data processing unit
- the interface to the host PC, including both a parallel port interface and a fiber optics link

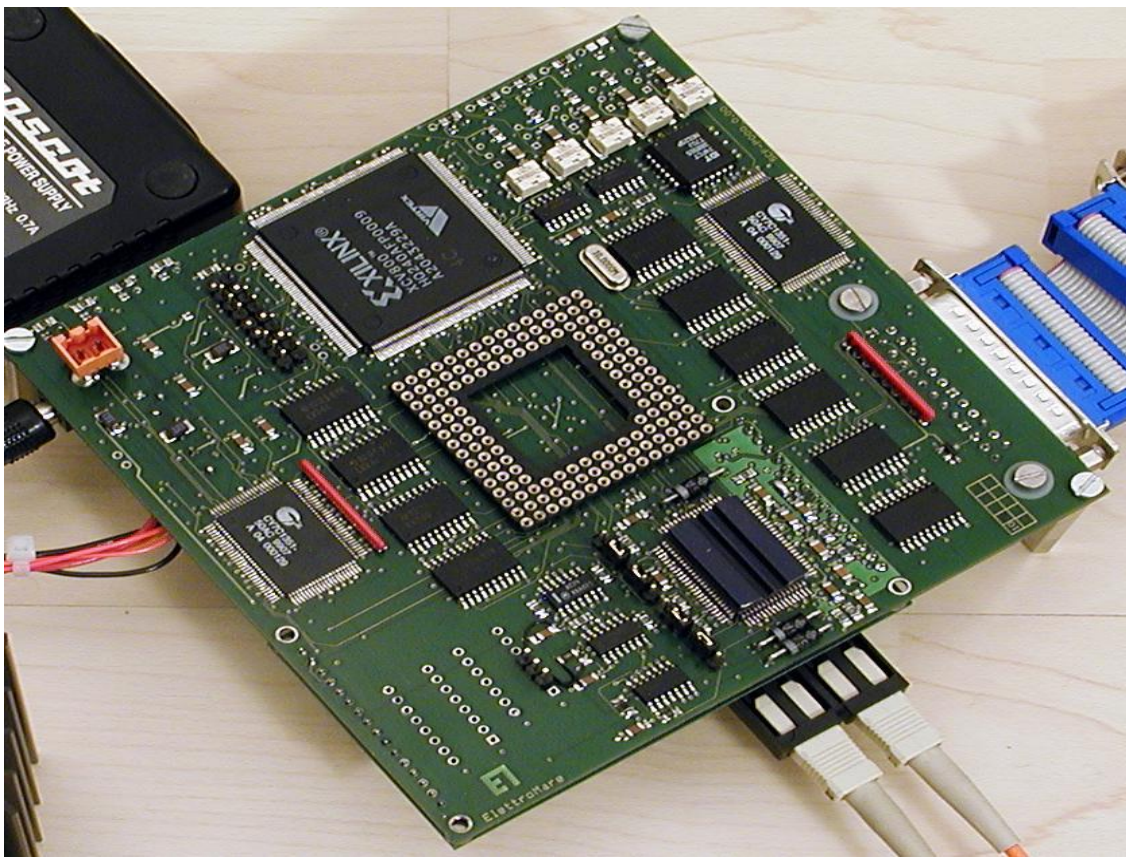


**Figure 2.** Electronics board (the APS socket is the central one).

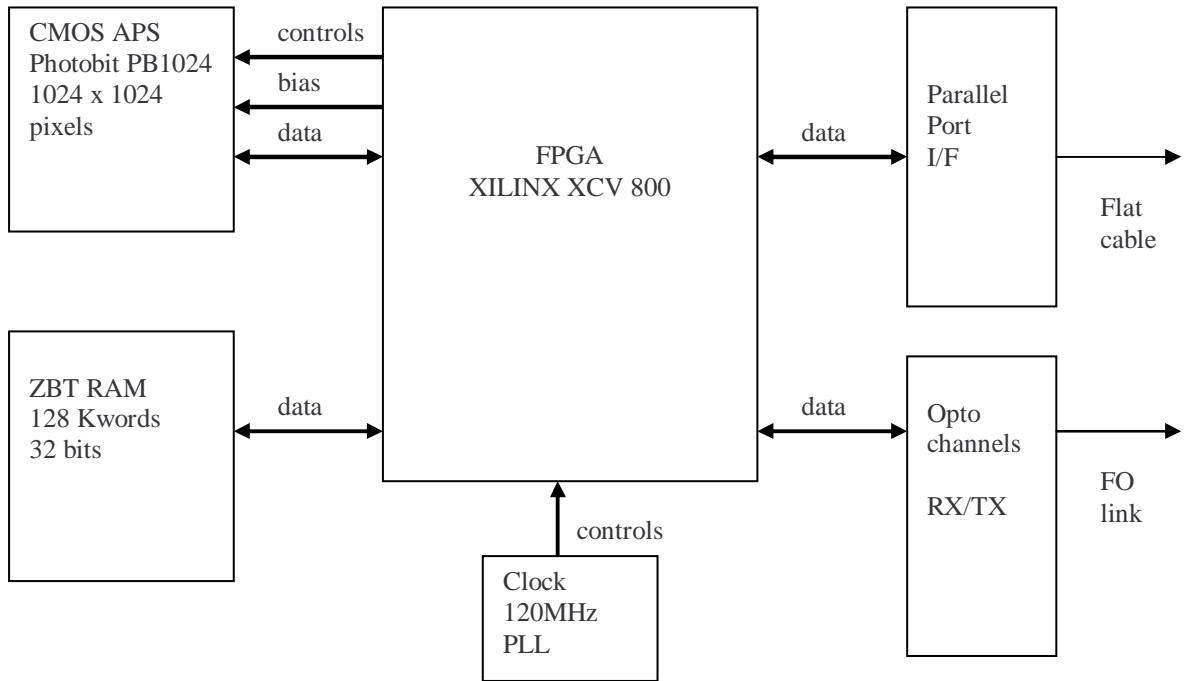


**Figure 3.** Block diagram of the PC-IAPS electronics.

The most part of the electronics needed to operate the APS as an imager is implemented on chip, including part of the timing and control circuitry and the AD converters. The row addressing, the bias signals and their telemetry, the data processing (i.e. event recognition and centroiding) and the interface to the host PC are all provided by the FPGA. A 128 Kwords 32 bit ZBT RAM is used to store the images to be subsequently readout at a slower data rate when the device is operated in frame grabber mode.

At each clock pulse, the 64 bits data output by the APS, corresponding to 8 pixels x 8-bit, are acquired by the data processor. By means of synchronous FIFO, the functions of shift registers connected in series are realized, to be fed by the APS readout system, which constitutes an effective delay line that allows a concurrent sampling of a pixel together with its nearest neighbors. Upon initialization, a set of D-Latches are used to map 8 windows of 3x3 pixels, which covers dynamically the whole APS image at the pace of the pixel clock. This allows the whole APS frame to be analyzed, avoiding problems of either fixed or dynamic image partitioning. The event recognition and centroid computation procedures are carried out simultaneously on all the 8 windows. A pipeline architecture allows to complete the elaboration of a 8 windows block every clock period, though the time required to carry out all the operations is several times longer, thus not limiting the dynamic performance of the detector.

#### 4. APS CAMERA CHARACTERIZATION

Before coupling the intensifier with the APS, we tested the APS camera (i.e.: APS and related controller) alone, operating the electronics in ‘frame grabber’ mode at different readout frequencies. For our photon counting application, we need the highest frame rate we can reach with acceptable performance in terms of linearity, noise, MTF.

##### 4.1 Linearity

We tested the linear response taking a series of flat field images at various integrating times. Each image has been dark-subtracted. The value of the signal, computed by averaging a 20 x 20 pixels region, is reported in fig.4 as a function of the exposure time. The camera response is linear to within 1% over the ADC dynamic range.

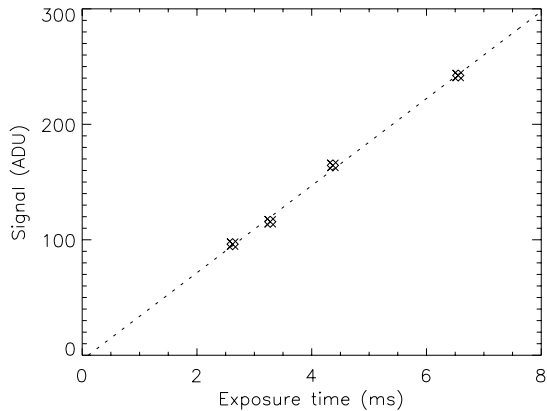


**Figure 4.** Linearity.

#### 4.2 Noise

Due to the high signal produced by the intensifier, a moderate readout noise does not significantly affect the signal-to-noise ratio of the detector, thus making the APS a good alternative to the most performant, but slower, CCD. The most relevant effect of the noise is the limitation of the spatial resolution achievable with the centroiding technique. However, as discussed in a previous paper<sup>13</sup>, a resolution able to resolve the pore structure of the Microchannel Plate can be obtained with a noise level reasonable for a high speed APS camera. Compatibly with that, we are interested in reaching the highest frame rate, since than it limits the dynamic range of the detector, even at the cost of a slightly higher noise.

A first evaluation of the performance in terms of noise at increasing readout frequency has been carried out taking a series of dark frames with different readout clocks. The main component of the noise, clearly apparent in Fig.5a, is a “column” Fixed Pattern Noise (FPN), most probably due to response variations among the ADCs (each column is readout by a different ADC). Fig.5b shows the same region after subtraction of the “column FPN”. The residual noise, especially at higher frame rate, is small (some kind of correction for the “column effect” could be easily introduced, if a better signal-to-noise ratio would be necessary).

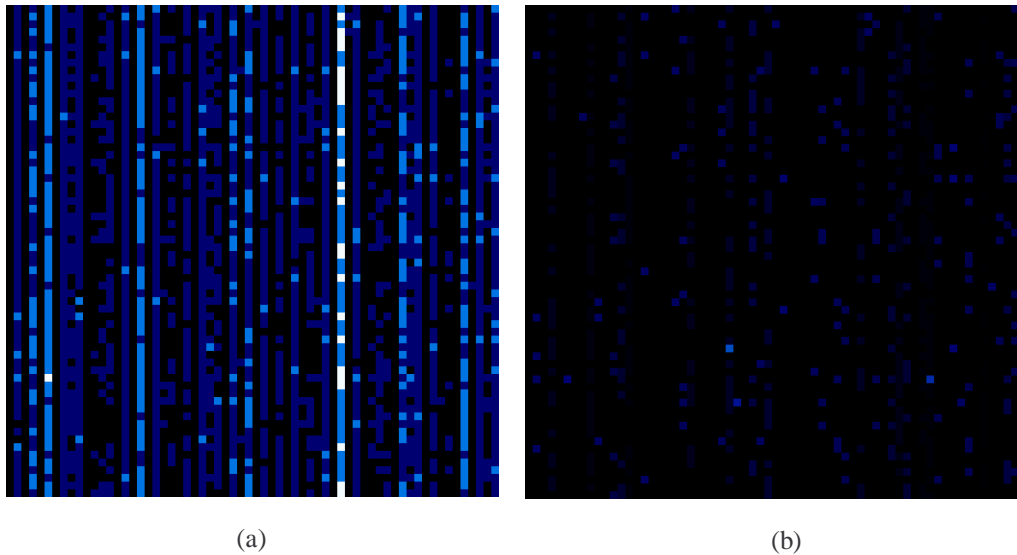


**Figure 5.** A region of a dark frame showing ‘column’ FPN (a) and a region after FPN subtraction (b)

However, up to clock frequency of about 40 MHz (corresponding to 320 frames/s full frame), the noise level is negligible, starting to sensibly increase only at 50 MHz (400 frame/s), close to the operative limit of the sensor (66 MHz). The plot in Fig.6 shows the rms noise on dark frames at different frame rates, before and after the correction for the FPN noise. The rms on the averaged column response is also reported.

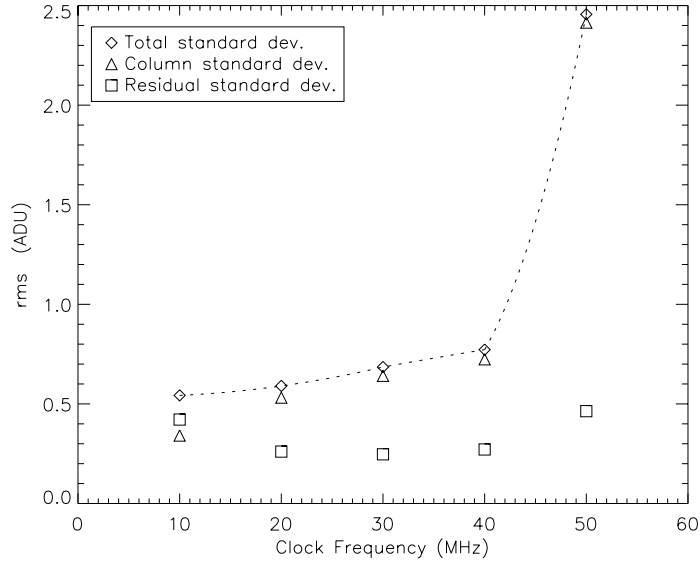


**Figure 6.** Rms noise on dark frames at different readout frequencies. The rms on raw frames is shown together with the rms after subtraction of the column FPN and the standard deviation of the column response.

### 4.3 Modulation Transfer Function

A standard USAF test target has been imaged in visible light onto the APS (Fig.7) by the relay optical system used for coupling the intensifier with the image sensor (i.e. the test target has been put at the place of the phosphor screen of the intensifier). The test target was illuminated by an incandescent lamp through a broadband filter peaked at 600 nm and with 100 nm FWHM band pass.

From the test target image the system Contrast Transfer Function (CTF) was evaluated, and transformed into the Modulation Transfer Function (MTF) according to the method described by Coltman<sup>16</sup>. The MTF obtained accounts for the APS intrinsic MTF together with the imaging optics contribution. No significant differences have been found changing the readout clock in the range 20-50 MHz.

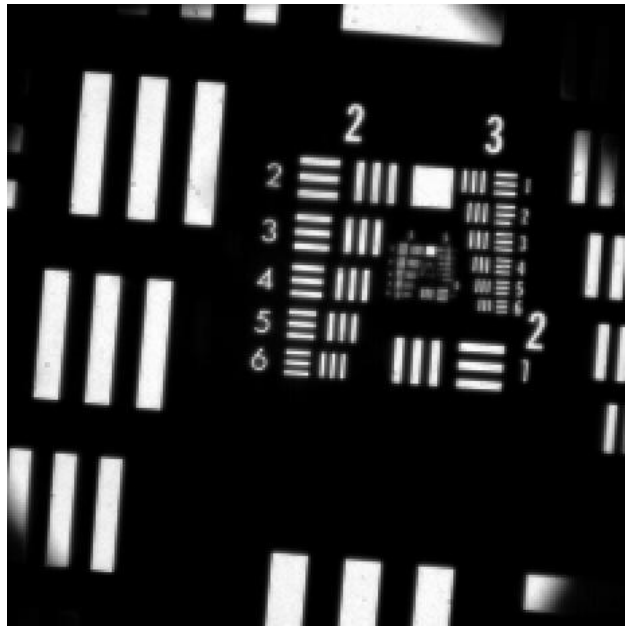


**Figure 7.** Image of the USAF Test Target

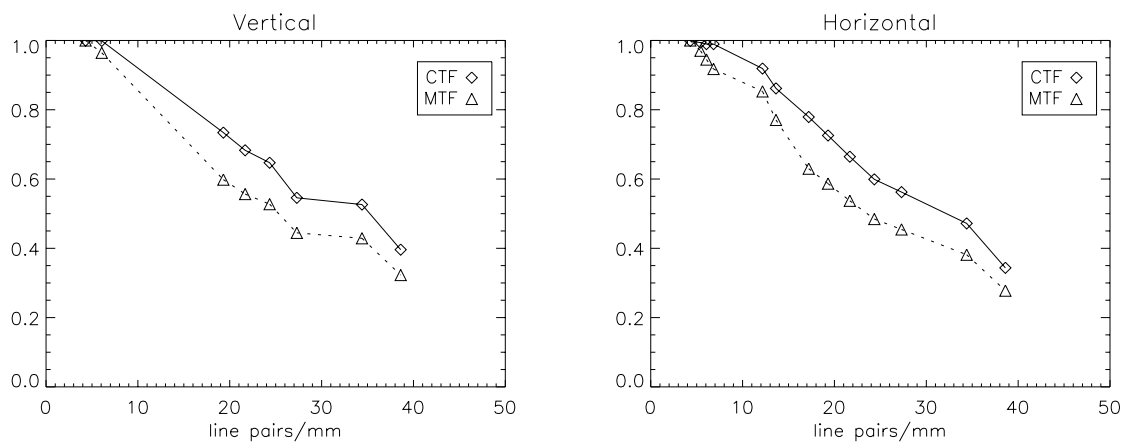


**Figure 8.** Contrast Transfer Function and Modulation Transfer Function for both directions.

#### 4 PHOTON EVENTS

After the APS tests, the intensifier has been coupled to the sensors. Before operating in centroiding mode, images of the photon events have been taken at different MCP gain in order to set the minimum MCP bias voltage required to detect events against the noise and to evaluate the threshold for event recognition. Unfortunately the maximum MCP gain is too low for a correct matching with the APS dynamic range. The peaks of the events hardly reach 30 ADU (on a 256 ADU range). However, the low background of the camera allows a moderate signal discrimination.

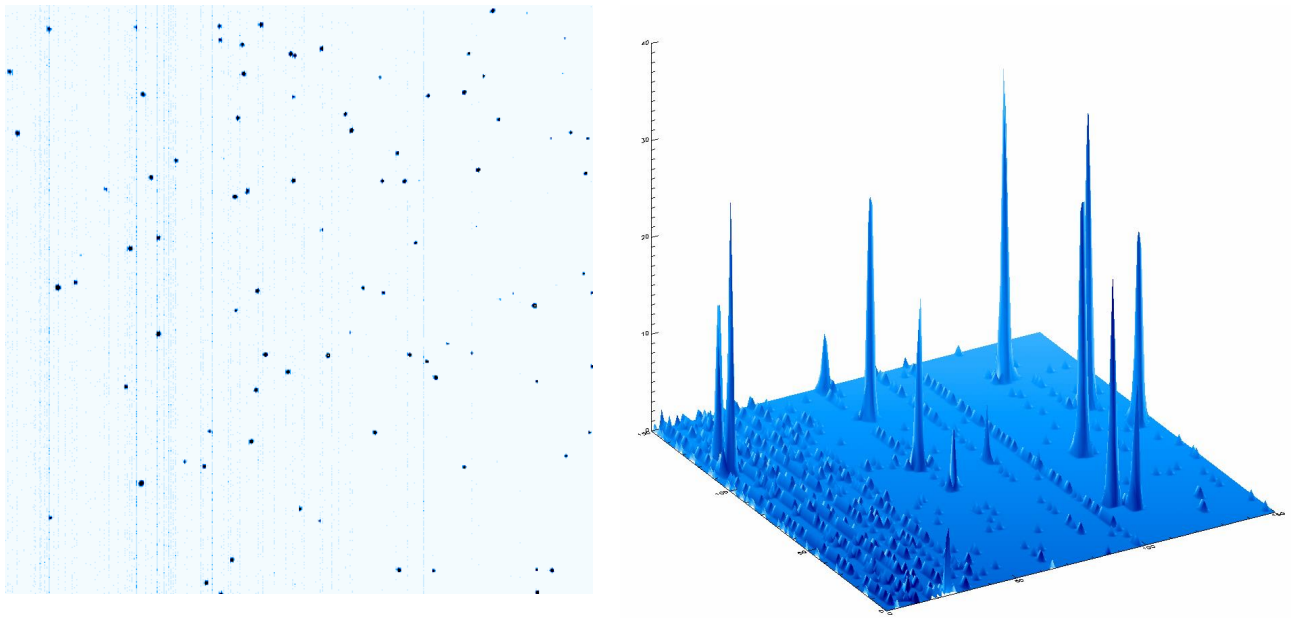


**Figure 9.** Image acquired at 20 MHz clock (160 frames/s) showing several photon events (spots) and 3D plot of a sub area.

The shape of the event is approximately gaussian (Fig.10), with  $\sigma \sim 0.7$  pixel in the x direction and  $\sigma \sim 0.8$  pixel in y, slightly larger than the optimum width for the 3-points center of gravity algorithm (about 0.5 pixel<sup>13</sup>).

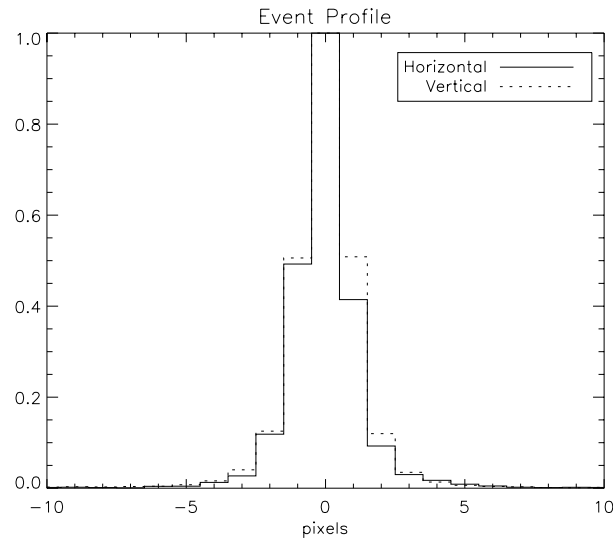


**Figure 10.** Profile of the sum of about 600 photon events.

## 6. EVENT RECOGNITION AND CENTROIDING

In order to test the data processing electronics with known patterns, we removed the intensifier and we used pinholes to simulate photon events on the APS. From the images taken in ‘frame grabber mode’ we were able to localize the peak of the simulated events in the pixel array. Then, switching the electronics in ‘centroiding mode’, we checked the location of the centroids computed from the electronics. First tests have been carried out with a single pinhole; eventually a mask with a regular grid has been used.

Fig.11 shows a comparison between the image of the same pinhole mask taken in direct imaging mode (left) and with event centroiding (right).

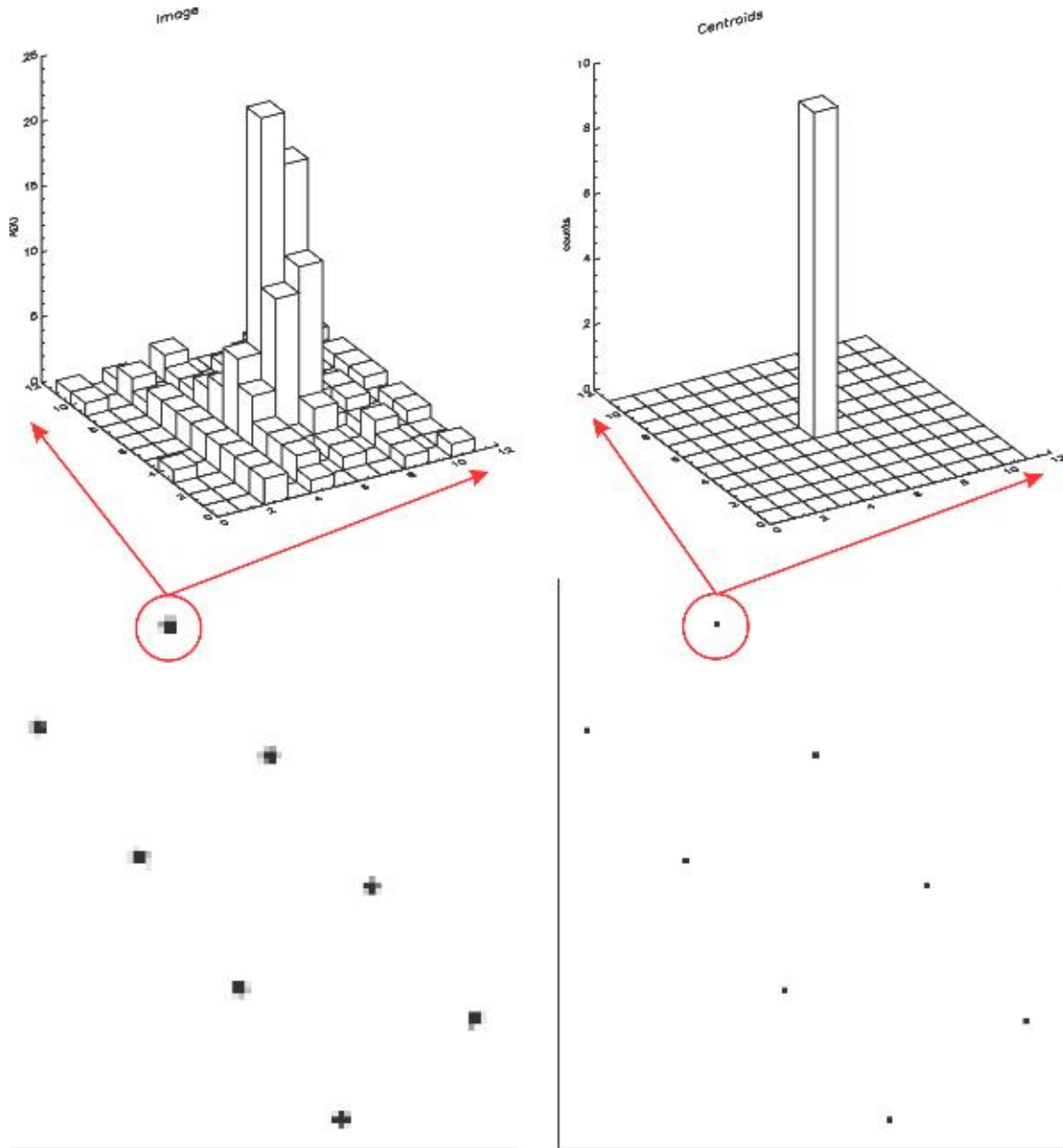


**Figure 11.** Image of a pinhole mask: (a) direct imaging, (b) reconstructed from event centroids (sampling: 1 bin/pixel).

## 7. CONCLUSIONS

We developed a new readout system based on CMOS APS for Microchannel Plate based photon-counting detector. The electronics is very compact, being implemented in a single 10 cm x 10 cm PCB board. We tested the device up to 50 MHz (400 frames/s 1024 x 1024 pixels, corresponding to 400 Mbytes/s of row data to be analyzed) without sensible reduction of the performance. This frame rate allows sustaining a point-like flux of about 80 counts/s with a loss of only 10%. Moreover, for this sensor, the frame rate is proportional to the inverse of the number of row to be read out, thus

reducing the field of view the dynamic range (and the time resolution) can improve of orders of magnitudes (or up to the intensifier limit).

## REFERENCES

1. O. H. W. Siegmund, M. Lampton, J. Bixler, S. Chakrabarti, J. Vallerga, S. Boyer, R. F. Malina,, *J. Opt. Soc. Am. A* **3**, p. 2139, 1986
2. M. Clampin and F. Paresce, *Astron. Astrophys.* **225**, p. 578, (1989)
3. O. H. W. Siegmund, M. Gummin, J. Stock, G. Naletto, G. Gaines, R. Raffanti, J. Hull, R. Abiad, T. Rodriguez-Bell, T. Magoncelli, P. Jelinsky, W. Donakowski, K. Kromer, *Proc. SPIE* **3114**, p. 283, (1997)
4. R. A. Kimble et al., *Astrophys. J.* **492**, L83, (1998)
5. J.L.A. Fordham, D.A. Bone, M.K.Oldfield, J.G.Bellis,T.J.Norton, *Proc.ESA SP-356*, p.103, (1992)
6. P. D. Read, I. G. van Breda, T. J. Norton, R. W. Airey, B. L. Morgan, J. R. Powell, *Instrumentation for Ground-Based Optical Astronomy, Present and Future*, ed. L. B. Robinson, Springer-Verlag N.Y.,p. 528, (1988)
7. M. K. Carter, B. E. Patchett, P. D. Read, N. Waltham, and I. G. van Breda, *NIM A* **310**, p. 305, (1991)
8. P.Bergamini, G.Bonelli, S.D'Angelo, S.Latorre, L.Poletto, G.Sechi E.G.Tanzi, G.Tondello, M.Uslenghi Proc. SPIE, **3114**, 250, (1997)
9. P.Bergamini, G.Bonelli, E.G.Tanzi, M.Uslenghi, L.Poletto, G.Tondello, *Review of Scientific Instruments*, **71**, n.4, 1841, (2000)
10. P.Bergamini, G.Bonelli, A.Paizis, L.Tommasi, M.Uslenghi, G.Tondello, R.Falomo, *Experimental Astronomy*, **10**, n.4, 457, (2000)
11. O.H. W. Siegmund, A.S. Tremsin, J.Vallerga, C.P.Beetz, R.W. Boerstler and D.Winn, *Proc. SPIE* **4497**
12. G.Bonanno, M.Belluso, A.Calì, C.Timpanaro, M.Uslenghi, M.Fiorini, A.Modica, *Proc. SPIE* **4498**
13. M.Uslenghi, G.Bonanno, M.Belluso, A.Modica, P.Bergamini, *Proc. SPIE* **4498**
14. C.Williams, Photobit, private communication
15. Photobit Corporation, PB-1024 Product Specification, August 1999
16. Coltman J.W., 1954, *JOSA*, **44**, 468